

Tuning the semiconducting nature of bis(phthalocyaninato) holmium complexes *via* peripheral substituents†Yanli Chen,^{*a} Dapan Li,^a Na Yuan,^a Jian Gao,^a Rongmin Gu,^a Guifen Lu^c and Marcel Bouvet^{*b}

Received 4th August 2012, Accepted 4th September 2012

DOI: 10.1039/c2jm35219b

The semiconducting properties of the heteroleptic and homoleptic bis(phthalocyaninato) holmium complexes bearing electron-withdrawing phenoxy substituents at the phthalocyanine periphery, namely Ho(Pc)[Pc(OPh)₈] (**1**) and Ho[Pc(OPh)₈]₂ (**2**) [Pc = unsubstituted phthalocyaninate; Pc(OPh)₈ = 2,3,9,10,16,17,23,24-octaphenoxyphthalocyaninate] have been investigated comparatively. Using a solution-based Quasi-Langmuir-Shäfer (QLS) method, the thin solid films of the two compounds were fabricated. The structure and properties of the thin films were investigated by UV-vis absorption spectra, X-ray diffraction (XRD) and atomic force microscopy (AFM). Experimental results indicated that H-type molecular stacking mode with the common preferential molecular “edge-on” orientation relative to the substrate has been formed, and the intermolecular face-to-face π - π interaction and film microstructures are effectively improve by increasing the number of phenoxy substituents of the Pc periphery within the double-decker complexes. The electrical conductivity of Ho(Pc)[Pc(OPh)₈] films was measured to be approximately 4 orders of magnitude larger than that of Ho[Pc(OPh)₈]₂ films, indicating significant effect of peripheral electron-withdrawing phenoxy groups on conducting behaviour of bis(phthalocyaninato) holmium complexes. In addition, the gas sensing behaviour of the QLS films of **1** and **2** toward electron donating gas, NH₃, was investigated in the concentration range of 15–800 ppm. Surprisingly, contrary responses towards NH₃ were found for the QLS films of **1** and **2**. In the presence of NH₃, the conductivity of the films of Ho(Pc)[Pc(OPh)₈] (**1**) decreased while the conductivity of the films of Ho[Pc(OPh)₈]₂ (**2**) increased. This observation clearly demonstrated the p- and n-type semiconducting nature for **1** and **2**, respectively. Furthermore, compared to the heteroleptic **1** having a hole mobility of $1.7 \times 10^{-4} \text{ cm}^2 \text{ V}^{-1} \text{ s}^{-1}$, homoleptic **2** exhibits an electron mobility as high as $0.54 \text{ cm}^2 \text{ V}^{-1} \text{ s}^{-1}$. Therefore, the inversion of the semiconducting nature of the double-deckers from p- to n-type can be successfully and easily realized just by increasing the number of peripheral phenoxy groups attached to the conjugated Pc cores.

Introduction

Organic field-effect transistors (OFETs) and chemical transducers with solution-processable organic semiconductors as active layers have attracted a significant research interest due to their potential applications in low-cost integrated circuits and flexible electronics.¹ Great progress has been achieved in the past decade towards developing novel semiconductor materials

especially those possessing π -conjugated electronic structure with high carrier mobility and good solubility in common organic solvents, such as conjugated polymers, oligomeric thiophenes, linear fused acenes, perylenes and phthalocyanines.² Compared with highly developed p-channel organic semiconductors, high-performance n-channel materials in particular those with solution processability still remains rare.^{3,4} Recently, an excellent n-type OFET based on solution-processable naphthalene diimide-thiophene copolymers with electron mobilities up to $0.85 \text{ cm}^2 \text{ V}^{-1} \text{ s}^{-1}$ was reported,⁵ which induces further incentive toward the fabrication of complementary circuits with enhanced performance and device operation.⁶

In the design of small molecular semiconductors, introduction of electron-deficient substituents has been proved to be an efficient way in lowering the molecular orbital energy and stabilizing the electron transport of semiconductors.^{6a,7-9} As exemplified by attaching strong electron-withdrawing groups such as F, Cl, or CN to the conjugated phthalocyanine (Pc) of phthalocyaninato

^aShandong Provincial Key Laboratory of Fluorine Chemistry and Chemical Materials, School of Chemistry and Chemical Engineering, University of Jinan, Jinan, China. E-mail: chm_chenyl@ujn.edu.cn

^bInstitut de Chimie Moléculaire de l'Université de Bourgogne, CNRS UMR 5260, Université de Bourgogne, Dijon, France. E-mail: marcel.bouvet@u-bourgogne.fr

^cSchool of Chemistry and Chemical Engineering, Jiangsu University, Zhenjiang, 212013, P.R. China

† Electronic supplementary information (ESI) available: HOMO and LUMO energies of compounds **1**–**2** estimated from cyclic voltammetry. See DOI: 10.1039/c2jm35219b

copper (CuPc), p-channel materials are able to be converted into n-channel semiconductors.¹⁰ However, these substituted CuPcs have to be fabricated into electronic devices (such as OFETs, chemical sensors) by means of vacuum deposition technique due to their low solubility in common organic solvents. The development of solution-processed n-type OFETs is still far behind that of the vacuum deposited devices. For example, the highest mobility of an evaporated C₆₀ thin-film is as high as 5 cm² V⁻¹ s⁻¹,¹¹ but the devices fabricated from a C₆₀ derivative by a solution process exhibits much inferior mobility of 0.1 cm² V⁻¹ s⁻¹.¹² Very recently, a Cu[Pc(COOC₈H₁₇)₈] complex bringing electron-withdrawing octyloxycarbonyl substituents at the phthalocyanine periphery by using solution-based self-assembly process was reported to show n-type nature with the carrier mobility for electron of ~10⁻⁴ cm² V⁻¹ s⁻¹.¹³ As a consequence, designing and synthesizing novel high performance n-type organic semiconducting materials with good solution processability remains a great challenge.

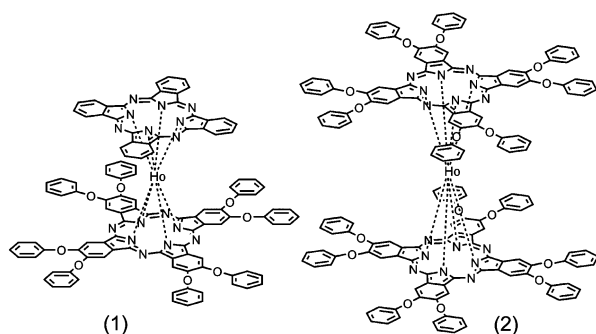
Bisphthalocyanines represent a special class of phthalocyanine-based molecular materials, which are sandwich complexes of rare earth elements (LnPc₂) and stable radical molecules. Guillaud and co-workers reported the thermally evaporated MPC₂ (M = Tm, Lu)-based OFETs with the mobility of 10⁻³ to 10⁻⁴ for holes obtained in air, and 10⁻⁴ to 10⁻⁵ cm² V⁻¹ s⁻¹ for electrons observed on C₁₈H₃₇SiCl₃ treated SiO₂/Si substrates in absence of air, respectively.¹⁴ On the other hand, the electron-withdrawing effect of phenoxy substituents has been evidenced in cyclic voltammetry experiments by Jiang *et al.*¹⁵ In light of these previous works, we report in this paper a new semiconductor family of heteroleptic and homoleptic bis(phthalocyaninato) holmium(III) complexes, namely Ho(Pc)[Pc(OPh)₈] (1) and Ho[Pc(OPh)₈]₂ (2) [Pc = unsubstituted phthalocyaninate; Pc(OPh)₈ = 2,3,9,10,16,17,23,24-octaphenoxyphthalocyaninate], Scheme 1. With a special sandwich structure and strong intermolecular π-π interactions between the phthalocyanine rings, this class of molecular materials are expected to be intrinsic semiconductors.¹⁶ In particular, introduction of electron-withdrawing phenoxy substituents onto the peripheral positions of the phthalocyanine ligand not only improves the solubility of the double-deckers in common organic solvents, but more importantly tunes the semiconducting nature of the double-deckers from p-type to novel n-type. With a hole mobility of 1.7 × 10⁻⁴ cm² V⁻¹ s⁻¹, OFET fabricated from Ho(Pc)[Pc(OPh)₈] (1) was observed to have p-type property. On the other hand, OFET made from Ho

[Pc(OPh)₈]₂ (2) displayed n-type property with an electron mobility of 0.54 cm² V⁻¹ s⁻¹, which is among the highest n-type mobility achieved thus far for solution-processed phthalocyanine-based OFET devices. The latter result highlights the significant effect of phenoxy substituents on the nature of bisphthalocyanine organic semiconductor. To the best of our knowledge, the present work also represents the first example of n-type solution-processed bisphthalocyanine-based OFET devices.

Results and discussion

Electronic absorption spectra

Electronic absorption spectra of 1–2 in chloroform and the QLS films were recorded and shown in Fig. 1. The spectra in chloroform solution are analogous to those reported for related homoleptic and heteroleptic bis(phthalocyaninato) rare earth compounds.^{15a,17–19} The spectra show the intense Soret bands in the range of 320–360 nm, and a Q-band, the most intense, at the 670 nm for 1, and 675 nm for 2 which has been attributed to a π-π* transition. The peaks found in the 470–490 nm region have been associated with a free radical structure of rare earth bisphthalocyanines.^{18,19} Compared to the spectra of heteroleptic Ho(Pc)[Pc(OPh)₈] in solution, the absorption spectra of Ho[Pc(OPh)₈]₂ showed red-shifted absorption bands as a result of the replacement of the second Pc ring by Pc(OPh)₈. This result implied that the optical transitions have significant contributions from the frontier molecular orbitals delocalized mainly on the two Pc rings, which makes them more susceptible to functionalization by attaching electron-withdrawing groups to the



Scheme 1 Schematic structures of bis(phthalocyaninato) holmium complexes 1–2.

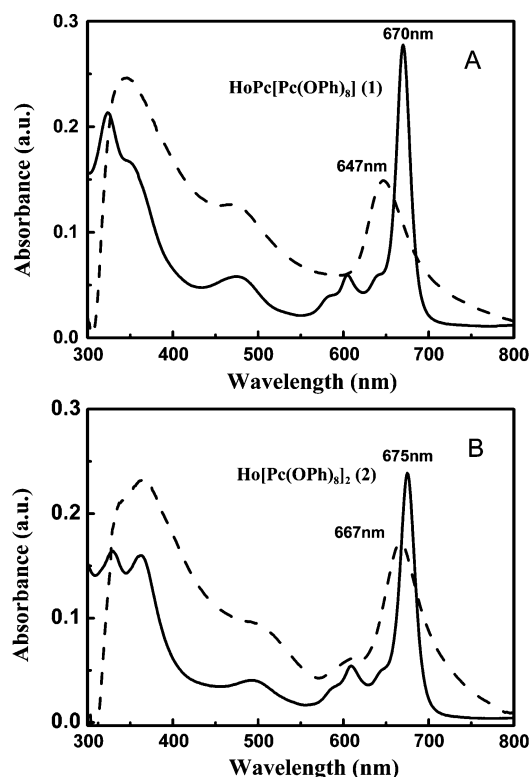


Fig. 1 UV-vis absorption spectra of compounds 1–2 (A and B) in dilute chloroform solution (solid line) and QLS films (dash line).

conjugated Pc cores.^{6a,20} In comparison with that of chloroform solution, the main Q band for the QLS films of the double-deckers was broadened and blue-shifted from 670 to 647 nm (23 nm) for **1**, from 675 to 667 nm (8 nm) for **2**. According to the exciton theory and previously published results,^{18,19,21} this blue shift indicates the formation of H-aggregates for both **1** and **2** in QLS films due to the face-to-face π - π interaction between bis(phthalocyaninato) rare earth double-deckers, which is believed to be a promising structural feature for charge-carrier transport.²² In addition, a remarkable red-shift of the Q band in QLS films of **2** compared to **1** was observed upon phenoxy functionalization, which is attributed to LUMO energetic stabilization arising from both the stronger electron-withdrawing ability and enhanced molecular ordering of the sixteen phenoxy substituents *versus* eight phenoxy substituents.^{6a} This conclusion is further confirmed by thin-film XRD, AFM and OFET measurement (*vide infra*).

X-Ray diffraction patterns

For most of the applications, the properties of the devices are closely related to the structure of solid films.²³ The quality of the thin solid films can be assessed using X-ray diffraction technique, which is helpful for understanding the microstructure-function relationship between molecular ordering in organic thin films and charge transport properties.⁹ Compounds **1–2** deposited on glass substrate give distinct diffraction peaks in their low angle region, Fig. 2, indicating that the molecules in the films are

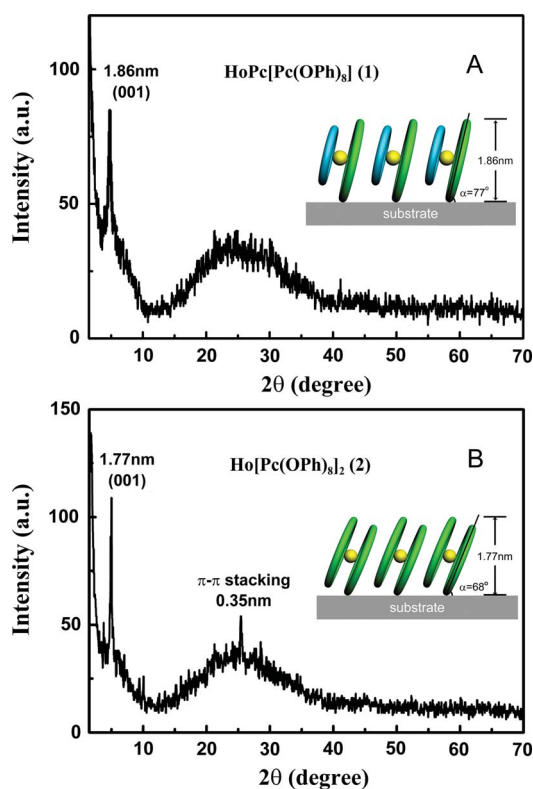


Fig. 2 X-Ray diffraction patterns of compounds **1–2** (A and B) QLS films on glass substrate. The inset of (A) and (B) shows schematic arrangement of **1** and **2** in QLS films, respectively.

uniformly oriented relative to the substrate plane.^{9,23} The XRD pattern of QLS films of **1** and **2** exhibits the (001) Bragg peak at $2\theta = 4.74^\circ$ and 4.98° , respectively, corresponding to a periodic spacing distance of 1.86 and 1.77 nm. As a consequence, orientation angles of phthalocyanine ring with respect to the substrate of 77° and 68° are estimated for **1** and **2** based on the diagonal dimension of $\text{Eu}[\text{Pc}(\text{OPh})_8]_2$ (1.91 nm) taken from single crystal X-ray diffraction result.^{15a} A slipped co-facial stacking mode was achieved for either **1** or **2** in the QLS films (the inset of Fig. 2A and B), which is consistent with their aggregation behaviours deduced from the electronic absorption spectroscopy. In addition, a high-order diffraction is found at 0.35 nm for $\text{Ho}[\text{Pc}(\text{OPh})_8]_2$ (**2**) films, which can be attributed to the π - π stacking distance among tetrapyrrole rings of double-decker molecules.²⁴ Such effective co-facial π - π stacking should be expected to decrease the barrier to charge transport, which in turn contributes to the excellent electron mobility revealed for the devices fabricated with **2** (*vide infra*). In the case of the films of **1**, only (001) diffraction peak is observed without the presence of an obvious π - π stacking feature, which would negatively impact on the carrier mobility, as discussed further below.

AFM surface topography

AFM provides more information on the aspect of the QLS films and therefore allows us to correlate the morphology and electrical properties. Fig. 3 compares the morphologies of the QLS films for double-deckers **1** and **2** deposited on the SiO_2/Si substrate. The surface of the QLS films of **1** presents a rod-like morphology of *ca.* 500–600 nm in length and 200–300 nm in width, giving a root mean square (rms) roughness value of 37.6, Fig. 3A, whereas that of **2** exhibits a granular structure with the average diameter of *ca.* 200–250 nm, Fig. 3B. A rms roughness value of 1.58 is achieved, indicating an especially smooth film of **2** covering the substrate. The more uniform grain size and much lower rms value for the QLS films of **2** compared to those of **1** is expected to cause fewer traps and/or defects localized around grain boundaries, and thus improving the carrier mobility.^{6c,25}

Current–voltage (*I–V*) characteristics

The electrical conductivity characterization of the QLS films of **1–2** based on a direct current–voltage (*I–V*) measurement was performed on insulating SiO_2 substrates with the ITO interdigitated electrodes. As shown in Fig. 4, two devices fabricated from the QLS films of **1–2** exhibit similar Ohmic behavior at low bias

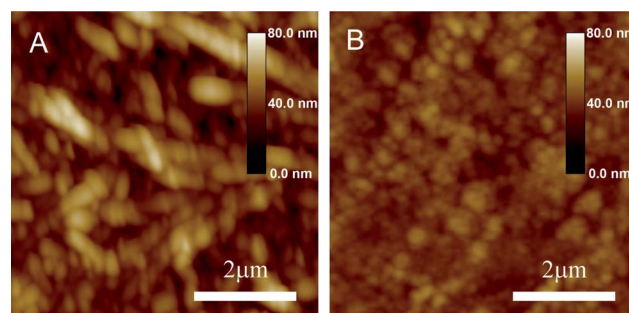


Fig. 3 AFM images of nanostructures of compounds **1–2** (A and B).

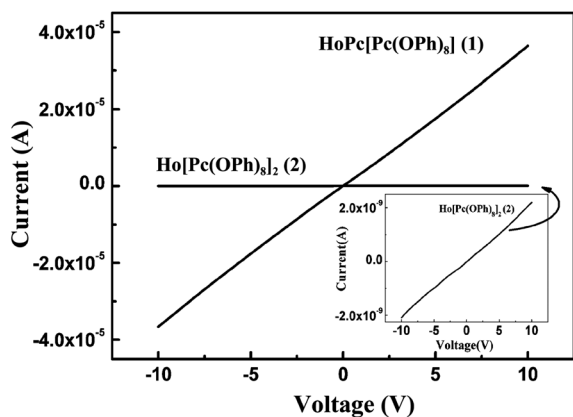


Fig. 4 Representative I - V characteristics for the QLS films of 1–2.

voltage. However, the response significantly decreases along with the increase in the number of phenoxy groups of the macrocycles from **2** to **1**. The devices exhibited the value of current in the order of 10^{-5} A for heteroleptic Ho(Pc)[Pc(OPh)₈] (**1**) and 10^{-9} A for homoleptic Ho[Pc(OPh)₈]₂ (**2**) under the bias of 10 V measured in air. The conductivity estimated is of the order of $\sim 10^{-4}$ and $\sim 10^{-8}$ S cm⁻¹ for the QLS films of **1** and **2**, respectively. Thus, there is a significant dependence on number of peripheral substituents for semiconducting films: Ho(Pc)[Pc(OPh)₈] (**1**) is about ten thousand times more conductive than Ho[Pc(OPh)₈]₂ (**2**). This trend in performance is consistent with the previously reported electrical behaviour of MPc and MPcF₁₆ (M = Cu, Zn) films since addition of electron-withdrawing substituents on a metallo phthalocyanine macrocycle decreases the electron density of the conjugated cycle and increases the oxidation potential of the macrocycle.^{26,27} This difference in the conductivity could also partly arise from different morphologies of the layers and from the presence of traps and/or defects (such as dopants). Much more traps and/or defects localized around grain boundaries in the QLS films of **1** than those of **2**, would be easier for trapping or creation of charge carriers, the concentration of which may be higher in the films of **1**.^{26,28}

Responses of Ho(Pc)[Pc(OPh)₈] and Ho[Pc(OPh)₈]₂ to NH₃

By comparing the first oxidation and the first reduction potentials of Ho(Pc)[Pc(OPh)₈] and Ho[Pc(OPh)₈]₂ reported in literature: $E_{\text{ox1}} = 0.56$ and 0.61 V; $E_{\text{red1}} = 0.12$ and 0.16 V vs. SCE, respectively,^{15a} it can be seen that Ho[Pc(OPh)₈]₂ is more easily reduced than Ho(Pc)[Pc(OPh)₈]; on the other hand, Ho(Pc)[Pc(OPh)₈] is more easily oxidized than Ho[Pc(OPh)₈]₂. To assess the applicability of differences in redox properties to gas sensing, the QLS films of **1–2** were exposed to different concentrations of electron-donating gas NH₃ (15–800 ppm) in an Ar atmosphere, with a duty cycle where the dynamic exposure period is fixed at 2 min and the recovery period at 5 min, at room temperature. Their conductivity variations are recorded, as shown in Fig. 5. As can be seen in Fig. 5A, the conductivity of compound **1** decreased during exposure and increased during recovery, exactly as expected for a p-type semiconductor, which is consistent with the sensing behavior reported previously on the unsubstituted analogue LuPc₂.²⁶ Upon exposure to the electron-donating gas,

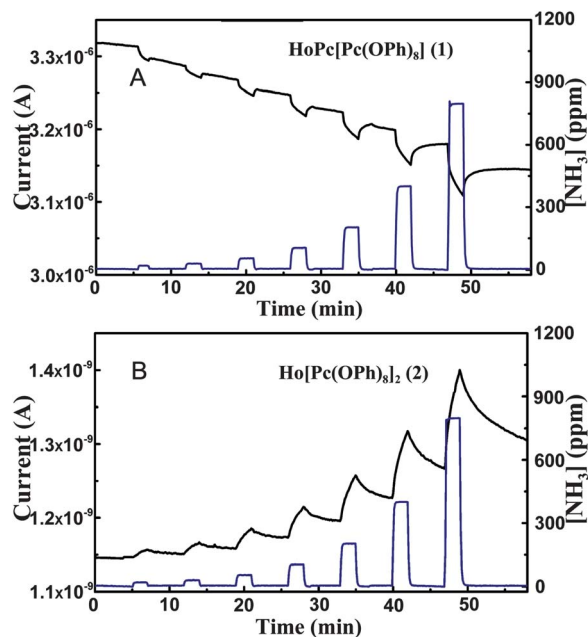


Fig. 5 The time-dependent current plots for (A) HoPc[Pc(OPh)₈] (**1**), and (B) Ho[Pc(OPh)₈]₂ (**2**) films exposed to NH₃ at varied concentration in the range of 15–800 ppm (exposure: 2 min, recovery: 5 min), while the bottom rectangular pulses for each current plot represent the NH₃ concentration as a function of time.

NH₃, the hole concentration near the surface of p-type semiconductor was expected to be reduced since NH₃ traps majority charge carriers, resulting in the decrease in conductivity. Surprisingly, for Ho[Pc(OPh)₈]₂ (**2**) the result was completely different, Fig. 5B. The conductivity increased in the presence of NH₃ and decreased in Ar. The similar behavior has already been observed in MPcs attached with electron-withdrawing groups.^{26,28} The current increase during exposure results from the creation of n-type charge carriers in the Ho[Pc(OPh)₈]₂ layer following charge transfer with the electron-donating gas NH₃. The sensing response to NH₃ of **1** and **2** unambiguously confirms that the majority carrier type inversion of the double-deckers from p- to n-type can be realized by varying the number of peripheral phenoxy substituents on the phthalocyanine ligands in a double-decker molecule.

In order to quantitatively analyze the sensor responses, the percent current change was calculated for each concentration, as follows using eqn (1):

$$\% \text{ current change} = [(I_0 - I_f)/I_0] \times 100 \quad (1)$$

where I_0 is the current value at the beginning of an exposure–recovery cycle and I_f is the current value at the end of the 2 min exposure period. That value is designated as the sensor response. As can be seen from Fig. 6, the sensor responses of the QLS films of **1–2** are all linear with respect to various concentrations of ammonia in the range of both 15–100 ppm and 200–800 ppm (Adj. R-squared > 0.97), respectively. For the QLS films of **1** and **2**, the slope (in % ppm⁻¹) of the linear fit of the percent current change as a function of NH₃ concentration, is about -0.0044 and 0.031 in the range of 15–100 ppm, and -0.0018 and 0.0089 in the range of 200–800 ppm, respectively. By comparison with the

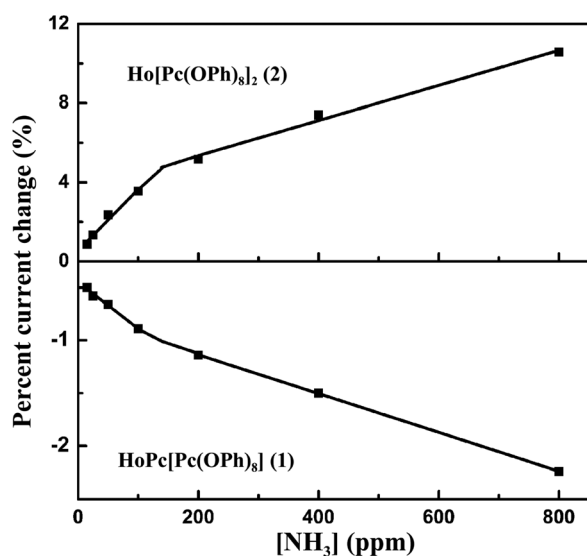


Fig. 6 Sensor response varies linearly with NH_3 concentration of the QLS films of compounds 1–2; the slope ($\% \text{ ppm}^{-1}$, $R^2 \geq 0.97$) for each may be used as a measure of sensor response.

absolute value of the slope, $\text{Ho}[\text{Pc}(\text{OPh})_8]_2$ is more sensitive to NH_3 than $\text{Ho}(\text{Pc})[\text{Pc}(\text{OPh})_8]$. This experiment is in agreement with the higher value of the reduction potential of $\text{Ho}[\text{Pc}(\text{OPh})_8]_2$ compared to $\text{Ho}(\text{Pc})[\text{Pc}(\text{OPh})_8]$, as determined by voltammetry measurement.^{15a} Thus, starting from a smaller current arising from the smaller conductivity, the QLS films of **2** offer a larger relative current increase (higher sensitivity) than those of **1**. This represents a promising way of improving the sensor response of organic materials to reducing gases.^{26,28,29} On the other hand, the time-dependent current plot of the QLS films of **2** shows a more clear separation of the different ammonia concentration levels and relatively better reversibility than that of **1**. The relatively uniform granular nanostructure with a densely packed molecular architecture and the lowest rms roughness value of the QLS films of **2** in this class of materials could partly contribute to the good sensing performance observed in our experiments. The lower sensitivity of largely rod-like surface morphology of **1**, as compared to that of the small-granular one of **2**, can then be explained by the difference in the number of adsorption sites. For the QLS films of **1**, continuity of the conductive path may be disrupted by a higher distribution of inter-space between the nanorods containing structural defects, with much of the NH_3 molecules adsorbed on the films having little contributions to the conductivity, thus the % current change is much smaller than that of **2**.³⁰ It is worth noting that, QLS films of **1–2** are very sensitive to low concentration NH_3 (15–100 ppm), which is important for the application as NH_3 sensor and/or detector in industrial wastes control.³⁰

OFET properties

To further investigate the majority carrier type and corresponding mobility of these double-deckers, typical top-contact/bottom-gate configuration OFET devices, in which the source and drain electrodes are vacuum-deposited on the top of the QLS films of **1–2**, have been fabricated. OFET properties were evaluated under

positive or negative gate bias in air/ N_2 to explore the majority charge carrier type, device performance, and environmental stability. Experimental data were analyzed using standard field-effect transistor equations: $I_{\text{ds}} = (W/2L)\mu C_0(V_{\text{g}} - V_{\text{th}})^2$, where I_{ds} is the source–drain current, V_{g} is the gate voltage, C_0 is the capacitance per unit area of the dielectric layer, and V_{th} is the threshold voltage, and μ is the mobility in the saturation region.³¹ The mobility (μ) and threshold voltage (V_{th}) can then be calculated from the slope and intercept of the linear part of the V_{g} vs. $(I_{\text{ds}})^{1/2}$ plot (at $V_{\text{ds}} = -40$ or 40 V, respectively). The QLS films of heteroleptic $\text{Ho}(\text{Pc})[\text{Pc}(\text{OPh})_8]$ (**1**) exhibit p-type characteristics in both air and N_2 with the carrier mobility for holes up to $1.7 \times 10^{-4} \text{ cm}^2 \text{ V}^{-1} \text{ s}^{-1}$ with an on–off ratio of $\sim 10^3$ and a threshold voltage of -21 V, Fig. 7A and B. It is worth noting that a negligible hole mobility change for the films of **1** was detected by changing the atmosphere, which should be related to its high density of intrinsic hole carriers in $\text{Ho}(\text{Pc})[\text{Pc}(\text{OPh})_8]$. As expected, no n-channel behavior was observed on bare SiO_2 in both air and N_2 , due to the unpassivated hydroxyl groups serving as electron traps,³² similar to the OFET behavior of the unsubstituted analogues MPC_2 ($\text{M} = \text{Tm}, \text{Lu}$) reported previously.¹⁴ As for n-type semiconductor, $\text{Ho}[\text{Pc}(\text{OPh})_8]_2$, we did not observe n-channel transistor behavior in air, perhaps due to atmospheric oxidants, such as water and oxygen.³³ However, inside the nitrogen glovebox, on un-treated substrates, n-channel behavior of **2** with the carrier mobility for electrons as high as $0.54 \text{ cm}^2 \text{ V}^{-1} \text{ s}^{-1}$ was observed (with an on–off ratio of $\sim 10^4$ and a threshold voltage of 12 V), Fig. 7C and D, which is among the highest electron mobility achieved to date for n-channel solution-processed phthalocyanine-based semiconductor.^{2,34} As a consequence, OFET majority carrier inversion from p- to n-type was realized just *via* tuning the number of peripheral electron-withdrawing phenoxy substituents introduced onto the phthalocyanine ligands for the first time. Note that compound **2** seems to represent also the first example of solution-processable n-type bisphthalocyanine-based semiconductor, to the best of our knowledge.

Investigations have revealed that the energy levels of the highest occupied molecular orbital (HOMO) and the lowest unoccupied molecular orbital (LUMO) are crucial in determining the majority charge carrier and charge carrier stability of organic semiconductors.^{35,36} In the present case, the HOMO and LUMO energy levels of **1–2** can be estimated from their half-wave potentials of the first and second reductions (*vs.* SCE) obtained by cyclic voltammetry.^{15a,37} As summarized in Table S1 (ESI†), both the HOMO and LUMO energy levels of -4.60 and -3.46 eV for $\text{Ho}[\text{Pc}(\text{OPh})_8]_2$ are lower than those of -4.56 and -3.42 eV for $\text{Ho}(\text{Pc})[\text{Pc}(\text{OPh})_8]$ due to the increase in the number of electron-withdrawing substituents for the former double-decker than the latter one, indicating that $\text{Ho}[\text{Pc}(\text{OPh})_8]_2$ (**2**) are harder to oxidize and easier to reduce than the analogous $\text{Ho}(\text{Pc})[\text{Pc}(\text{OPh})_8]$ (**1**).^{20,37,38} In addition, LUMO stabilization with a greater magnitude in thin-film for **2** than **1** from nonsymmetric decreases in the thin-film HOMO and LUMO energies confirmed by red-shift of optical band gap should be highly responsible for the difference on the behaviors of OFETs between compounds **2** and **1**. However, the fact that the n-type semiconductor property of the QLS films of **2** was detected only under inert atmosphere suggests that the LUMO energy of **2** in QLS films still does not meet the requirement for an air-stable n-type OFETs, which

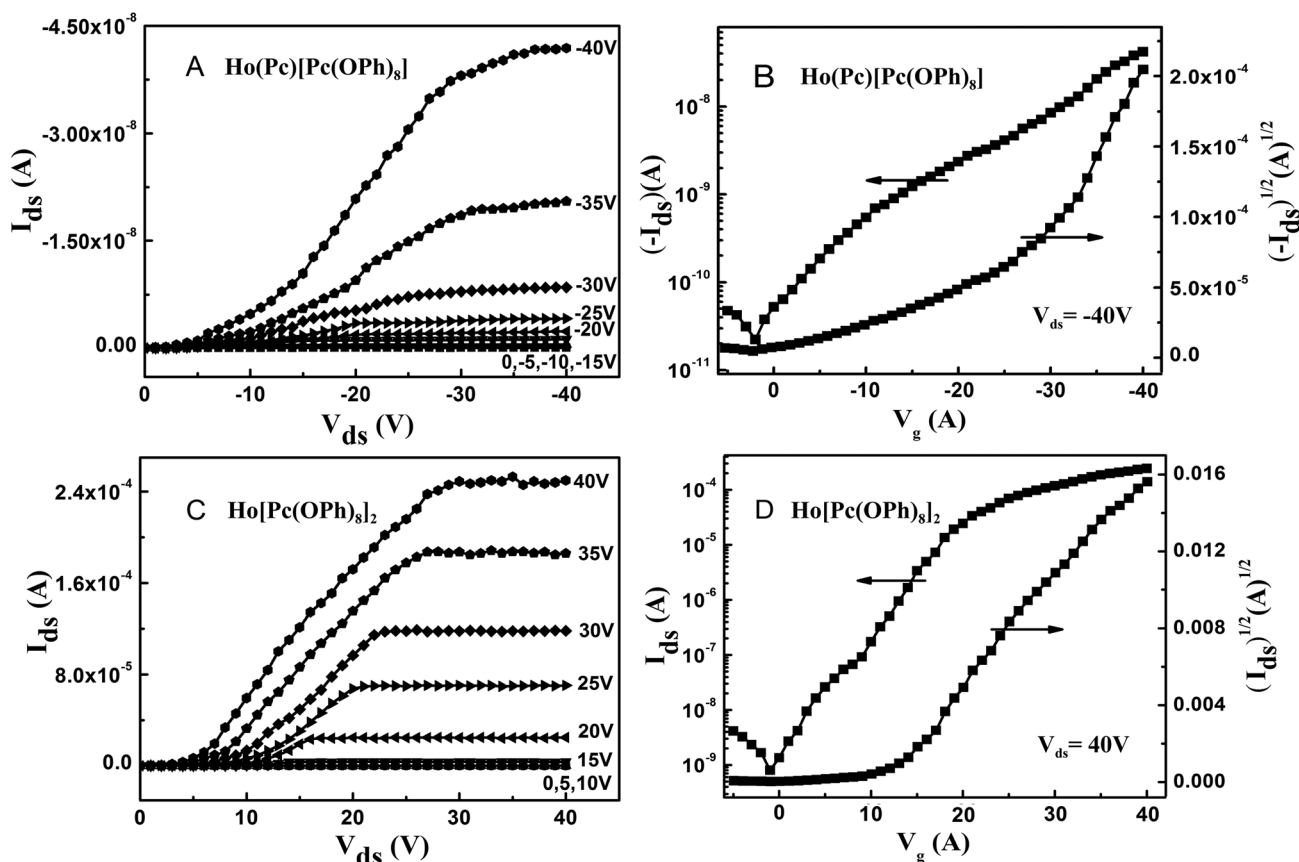


Fig. 7 Drain-source current (I_{ds}) versus drain-source voltage (V_{ds}) characteristic at different gate voltage (left) and transfer curve (right) for **1** (A and B) in air and **2** (C and D) in N₂, respectively, on the un-treated SiO₂/Si substrates.

demands the value of LUMO energy lower than -4.0 eV to against the air-derived electron traps.^{9,39}

Conclusions

In summary, the semiconducting properties of the heteroleptic and homoleptic bis(phthalocyaninato) holmium complexes have been comparatively investigated. Optical and electrochemical data demonstrate that HOMO/LUMO energies can be tuned *via* phenoxy group introduction onto the bisphthalocyanines. The UV-vis absorption spectra, XRD and AFM images of QLS films of **1** and **2** revealed more effective face-to-face π - π interactions and organized film microstructures in the film of **2**. The inverted current responses towards NH₃ for the device of Ho(Pc)[Pc(OPh)₈] (**1**) and Ho[Pc(OPh)₈]₂ (**2**) unambiguously demonstrated the p- and n-type semiconducting nature for **1** and **2**, respectively. Correlatively, the sensitivity of **2** to NH₃ is much higher than that of **1**. Furthermore, OFET of **1** shows carrier mobility of $1.7 \times 10^{-4} \text{ cm}^2 \text{ V}^{-1} \text{ s}^{-1}$ for holes and that of **2** displays carrier mobility as high as $0.54 \text{ cm}^2 \text{ V}^{-1} \text{ s}^{-1}$ for electrons. The latter is among the highest n-type mobility achieved thus far for solution-processed phthalocyanine-based OFET devices. In particular, the majority carrier inversion from p- to n-type was successfully and easily realized just by tuning the number of peripheral electron-withdrawing phenoxy groups in the double-decker molecules. The good performance proves that

these bis(phthalocyaninato) rare earth double-deckers are very promising organic semiconductors. The design and synthesis of air-stable n-type semiconducting materials based on new sandwich-type tetrapyrrolo rare earth complexes with good solubility in organic solvents are being developed in our lab.

Experimental

Chemicals

Bis(phthalocyaninato) rare earth(III) complexes **1–2** were synthesized according to a previously published procedure.^{15a} All other reagents and solvents were of reagent grade and used as received.

Characterization

Electronic absorption spectra were recorded on a Hitachi U-4100 spectrophotometer. X-Ray diffraction experiment was carried out on a Rigaku D/max-B X-ray diffractometer. AFM images were collected in air under ambient conditions using the tapping mode with a NanoscopeIII/Bioscope scanning probe microscope from Digital instruments.

Electrical measurements

The fundamental electrical measurements for the QLS films of **1–2** deposited onto interdigitated electrodes array were

performed using a Keithley 6517 electrometer with an incorporated DC voltage supply. The electrometer is controlled by self-made software via the GP-IB board. Current–voltage (I – V) curves were registered in the -10 to 10 V voltage range with 1 V increments, starting and finishing at 0 V bias to avoid irreversible polarization effects. On the other hand, the NH_3 -sensing properties of samples have been examined by exposing the corresponding films to different concentrations of ammonia and measuring the current changes of the films at a constantly polarized voltage of 5 V. All experiments have been conducted at least twice to ensure reproducibility. The interdigitated electrode array is composed of 10 pairs of ITO electrode digits (fingers) deposited onto a glass substrate with the following dimensions: 125 μm electrode width, 75 μm spacing, 5850 μm overlapping length, and 20 nm electrode thickness. QLS films were prepared following the method published previously.³⁰ In the present case, the 20-layer QLS films of 1–2 were obtained for electrical measurements.

Gas sources for sensing experiments

The desired ammonia concentration was produced by diluting a mixture NH_3/Ar (1000 ppm NH_3 , from Air Liquid, France) with dry Ar using two mass flow controllers (total mass flow: 0.5 L min^{-1}). The maximum water contents in ammonia and argon cylinders purchased were 100 ppm and 2 ppm respectively.

OTFT device fabrication

OTFT devices were fabricated on a Si/SiO_2 (300 nm thickness, capacitance $C_0 = 10$ nF cm^{-2}) substrate by evaporating gold electrodes onto the QLS films of 1–2 employing a shadow mask. These electrodes have a channel width (W) of 28.6 mm and a channel length (L) of 0.24 mm. The ratio of the width to length (W/L) of the channel was then 119 . The drain–source current (I_{ds}) versus drain–source voltage (V_{ds}) characteristic was obtained with a Hewlett–Packard (HP) 4140B parameter analyzer at room temperature.

Acknowledgements

The authors would like to thank the Natural Science Foundation of China (20871055) and the Natural Science Foundation of Shandong Province (ZR2011BZ005) for the financial support of this work. The authors thank the Conseil Régional de Bourgogne for funding through the program PARI SMT 08 SME – Région Bourgogne.

Notes and references

- (a) C. D. Dimitrakopoulos and P. R. L. Malenfant, *Adv. Mater.*, 2002, **14**, 99; (b) G. Horowitz, *Adv. Mater.*, 1998, **10**, 365; (c) H. Sirringhaus, *Adv. Mater.*, 2005, **17**, 2411; (d) R. Li, W. Hu, Y. Liu and D. Zhu, *Acc. Chem. Res.*, 2010, **43**, 29; (e) H. Usta, A. Facchetti and T. J. Marks, *Acc. Chem. Res.*, 2011, **44**, 501; (f) L. Valli, *Adv. Colloid Interface Sci.*, 2005, **116**, 13.
- (a) W. Wu, Y. Liu and D. Zhu, *Chem. Soc. Rev.*, 2010, **39**, 1489; (b) R. P. Ortiz, A. Facchetti and T. J. Marks, *Chem. Rev.*, 2010, **110**, 205; (c) S. Liu, W. M. Wang, A. L. Briseno, S. C. B. Mannsfeld and Z. Bao, *Adv. Mater.*, 2009, **21**, 1217; (d) Y. Wang, Y. Chen, R. Li, S. Wang, X. Li and J. Jiang, *Langmuir*, 2007, **23**, 5836.
- C. R. Newman, C. D. Frisbie, D. A. da Silva, J. L. Bredas, P. C. Ewbank and K. R. Mann, *Chem. Mater.*, 2004, **16**, 4436.
- (a) J. Zaumseil and H. Sirringhaus, *Chem. Rev.*, 2007, **107**, 1296; (b) A. Facchetti, *Mater. Today*, 2007, **10**, 28.
- (a) Z. Chen, Y. Zheng, H. Yan and A. Facchetti, *J. Am. Chem. Soc.*, 2009, **131**, 8; (b) H. Yan, Z. Chen, Y. Zheng, C. Newman, J. R. Quinn, F. Dötz, M. Kastler and A. Facchetti, *Nature*, 2009, **457**, 67.
- (a) H. Usta, C. Risko, Z. Wang, H. Huang, M. K. Deliomeroğlu, A. Zhukhovitskiy, A. Facchetti and T. J. Marks, *J. Am. Chem. Soc.*, 2009, **131**, 5586; (b) B. Crone, A. Dodabalapur, Y.-Y. Lin, R. W. Filas, Z. Bao, A. LaDuca, R. Sarpeshkar, H. E. Katz and W. Li, *Nature*, 2000, **403**, 521; (c) M. M. Durban, P. D. Kazarinoff and C. K. Luscombe, *Macromolecules*, 2010, **43**, 6348.
- A. Facchetti, M. H. Yoon, C. L. Stern, G. R. Hutchison, M. A. Ratner and T. J. Marks, *J. Am. Chem. Soc.*, 2004, **126**, 13480.
- M. H. Yoon, S. A. DiBenedetto, A. Facchetti and T. J. Marks, *J. Am. Chem. Soc.*, 2005, **127**, 1348.
- B. A. Jones, A. Facchetti, M. R. Wasielewski and T. J. Marks, *J. Am. Chem. Soc.*, 2007, **129**, 15259.
- (a) Z. Bao, A. J. Lovinger and J. Brown, *J. Am. Chem. Soc.*, 1998, **120**, 207; (b) M. L. Tang, J. H. Oh, A. D. Reichardt and Z. Bao, *J. Am. Chem. Soc.*, 2009, **131**, 3733; (c) D. Schlettwein, D. Wohlr, E. Karmann and U. Melville, *Chem. Mater.*, 1994, **6**, 3.
- Y. Ito, A. A. Virkar, S. Mannsfeld, J. H. Oh, M. Toney, J. Locklin and Z. Bao, *J. Am. Chem. Soc.*, 2009, **131**, 9396.
- P. H. Wobkenberg, D. D. C. Bradley, D. Kronholm, J. C. Hummelen, D. M. de Leeuw, M. Colle and T. D. Anthopoulos, *Synth. Met.*, 2008, **158**, 468.
- P. Ma, J. Kan, Y. Zhang, C. Hang, Y. Bian, Y. Chen, N. Kobayashi and J. Jiang, *J. Mater. Chem.*, 2011, **21**, 18552.
- G. Guillaud, M. A. Sadoun, M. Maitrot, J. Simon and M. Bouvet, *Chem. Phys. Lett.*, 1990, **167**, 503.
- (a) G. Lu, M. Bai, R. Li, X. Zhang, C. Ma, P.-C. Lo, D. K. P. Ng and J. Jiang, *Eur. J. Inorg. Chem.*, 2006, **18**, 3703; (b) R. Li, X. Zhang, P. Zhu, D. K. P. Ng, N. Kobayashi and J. Jiang, *Inorg. Chem.*, 2006, **45**, 2327.
- (a) P. Turek, P. Petit, J.-J. André, R. Even, B. Boudjema, G. Guillaud and M. Maitrot, *J. Am. Chem. Soc.*, 1987, **109**, 5119; (b) M. Bouvet, in *The Porphyrin Handbook*, ed. K. M. Kadish, R. Guilard and K. Smith, Academic Press, Oxford, 2003, vol. 19.
- W. Su, M. Bao and J. Jiang, *Vib. Spectrosc.*, 2005, **39**, 186.
- D. Markovitsi, T. H. Tran-Thi, R. Even and J. Simon, *Chem. Phys. Lett.*, 1987, **137**, 107.
- M. L. Rodríguez-Méndez, Y. Gorbunova and J. A. de Saja, *Langmuir*, 2002, **18**, 9560.
- Y. Zhang, X. Cai, Y. Zhou, X. Zhang, H. Xu, Z. Liu, X. Li and J. Jiang, *J. Phys. Chem. A*, 2007, **111**, 392.
- M. Kasha, H. R. Rawls and M. A. El-Bavoumi, *Pure Appl. Chem.*, 1965, **11**, 371.
- X. Mu, W. Song, Y. Zhang, K. Ye, H. Zhang and Y. Wang, *Adv. Mater.*, 2010, **22**, 4905.
- (a) Y. Chen, W. Su, M. Bai, J. Jiang, X. Li, Y. Liu, L. Wang and S. Wang, *J. Am. Chem. Soc.*, 2005, **127**, 15700; (b) W. Su, J. Jiang, K. Xiao, Y. Chen, Q. Zhao, G. Yu and Y. Liu, *Langmuir*, 2005, **21**, 6527; (c) R. Li, P. Ma, S. Dong, X. Zhang, Y. Chen, X. Li and J. Jiang, *Inorg. Chem.*, 2007, **46**, 11397; (d) Y. Gao, P. Ma, Y. Chen, Y. Zhang, Y. Bian, X. Li, J. Jiang and C. Ma, *Inorg. Chem.*, 2009, **48**, 45; (e) J. Simon and P. Bassoul, *Design of Molecular Materials: Supramolecular Engineering*, John Wiley & Sons, London and New York, 2001.
- (a) G. Lu, Y. Chen, Y. Zhang, M. Bao, Y. Bian, X. Li and J. Jiang, *J. Am. Chem. Soc.*, 2008, **130**, 11623; (b) Y. Gao, X. Zhang, C. Ma, X. Li and J. Jiang, *J. Am. Chem. Soc.*, 2008, **130**, 17044.
- T. Lee, C. A. Landis, B. M. Dhar, B. J. Jung, J. Sun, A. Sarjeant, H.-J. Lee and H. E. Katz, *J. Am. Chem. Soc.*, 2009, **131**, 1692.
- V. Parra, J. Brunet, A. Pauly and M. Bouvet, *Analyst*, 2009, **134**, 1776.
- (a) Z. Bao, A. J. Lovinger and A. Dodabalapur, *Appl. Phys. Lett.*, 1996, **69**, 3066; (b) D. G. De Oteyza, E. Barrera, J. O. Osso, S. Sellner and H. Dosch, *J. Am. Chem. Soc.*, 2006, **128**, 15052; (c) R. Murdey, N. Sato and M. Bouvet, *Mol. Cryst. Liq. Cryst.*, 2006, **455**, 211.
- B. Schöllhorn, J. P. Germain, A. Pauly, C. Maleysson and J. P. Blanc, *Thin Solid Films*, 1998, **326**, 245.
- (a) M. Passard, A. Pauly, J. P. Germain and C. Maleysson, *Synth. Met.*, 1996, **80**, 25; (b) A. Giraudeau, H. J. Callot, J. Jordan, I. Ezhar and M. Gross, *J. Am. Chem. Soc.*, 1979, **101**, 3857; (c) A. Kempa, *Synth. Met.*, 1993, **59**, 231; (d) A. Louati, M. El Meray,

- J. J. André, J. Simon, K. M. Kadish, M. Gross and A. Giraudeau, *Inorg. Chem.*, 1985, **24**, 1175; (e) L. G. Pakhomov and G. L. Pakhomov Jr, *Synth. Met.*, 1995, **71**, 2299; (f) B. Timmer, W. Olthuis and A. van den Berg, *Sens. Actuators, B*, 2005, **107**, 666.
- 30 (a) Y. Chen, M. Bouvet, T. Sizun, Y. Gao, C. Plassard, E. Lesniewska and J. Jiang, *Phys. Chem. Chem. Phys.*, 2010, **12**, 12851; (b) J. Gao, G. Lu, J. Kan, Y. Chen and M. Bouvet, *Sens. Actuators, B*, 2012, **166–167**, 500.
- 31 S. M. Sze, in *Physics of Semiconductor Devices*, John Wiley & Sons, New York, 1981.
- 32 M. L. Tang, A. D. Reichardt, N. Miyaki, R. M. Stoltenberg and Z. Bao, *J. Am. Chem. Soc.*, 2008, **130**, 6064.
- 33 T. D. Anthopoulos, G. C. Anyfantis, G. C. Papavassiliou and D. M. de Leeuw, *Appl. Phys. Lett.*, 2007, **90**, 122105.
- 34 L. Zhang, C. Di, G. Yu and Y. Liu, *J. Mater. Chem.*, 2010, **20**, 7059.
- 35 (a) A. Facchetti, M. Musherush, M.-H. Yoon, G. R. Hutchison, M. A. Ratner and T. J. Marks, *J. Am. Chem. Soc.*, 2004, **126**, 13859; (b) G. R. Hutchison, M. A. Ratner and T. J. Marks, *J. Am. Chem. Soc.*, 2005, **127**, 16866; (c) G. R. Hutchison, M. A. Ratner and T. J. Marks, *J. Am. Chem. Soc.*, 2005, **127**, 2339.
- 36 A. Facchetti, M. Musherush, H. E. Katz and T. J. Marks, *Angew. Chem., Int. Ed.*, 2003, **15**, 33.
- 37 P. Zhu, F. Lu, N. Pan, D. P. Arnold, S. Zhang and J. Jiang, *Eur. J. Inorg. Chem.*, 2004, **3**, 510.
- 38 R. Murdey, M. Bouvet, M. Sumimoto, S. Sakaki and N. Sato, *Synth. Met.*, 2009, **159**, 1677.
- 39 Z. Wang, C. Kim, A. Facchetti and T. J. Marks, *J. Am. Chem. Soc.*, 2007, **129**, 13362.